10,11

Effect of Excess Hydrogen Flow in Reactor on PECVD Growth of Carbon Nanotubes

© S.V. Bulyarskiy, M.S. Molodenskiy, P.E. Lvov, A.A. Pavlov, Yu.V. Anufriev, Yu.P. Shaman, G.G. Gusarov, K.A. Modestov, A.V. Sysa, A.P. Shevchenko

Institute of Nanotechnology of Microelectronics, Russian Academy of Sciences, Moscow, Russia

E-mail: bulyar2954@mail.ru

Received January 10, 2025
Revised January 10, 2025
Accepted January 11, 2025

The paper studies the effect of hydrogen flow on vapor-phase synthesis of carbon nanotubes in gas discharge plasma. Increasing the hydrogen flow in the reactor reduces the plasma temperature and increases the number of defects in the synthesized nanotubes. Analysis of the thermodynamics of synthesis shows that increasing the hydrogen concentration reduces the activity of the catalyst and reduces the amount of carbon supplied to the growing nanotube, which leads to an increase in the number of defects.

Keywords: carbon nanotubes, synthesis, defects.

DOI: 10.61011/PSS.2025.02.60686.8-25

1. Introduction

Carbon nanotubes (CNT) are a promising material for many technologically important applications [1,2]. They are used for making field emission cathodes employed in the development of miniature tubes, X-ray sources [2,3], microwave band amplifiers [4], display units [5]. These applications require CNT with particular properties, including a desired length, diameter and substrate packing density. Growth conditions for CNT with such properties are being studied extensively. CNT crystal structure, chirality, diameter and growth rates depend on the type of catalyst and growth technique.

Chemical vapor deposition (CVD) and plasma-enhanced CVD (PECVD) of carbon nanotubes have been increasingly used recently. Due to the inclusion of plasma into the growth process, synthesis goes at a lower substrate temperature. This is provided by an additional plasma power source that facilitates precursor dissociation and ensures improved control of CNT properties such as chirality, length and diameter [6–9]. However, the effect of gas mixture composition in the reactor on the quality of grown CNT is still insufficiently understood. Therefore, the objective of this paper is to study the effect of hydrogen flow rate in the reactor on the CNT growth.

2. Test samples

2.1. Catalyst preparation

Iron was used as a catalyst of CNT array growth. Iron particles on the silicon oxide surface were formed by a spray technique. For this, an iron nitrate solution ($Fe(NO_3)_2 \cdot 9H_2O$) in isopropyl alcohol was used. $Fe(NO_3)_2 \cdot 9H_2O$ concentration in the solution was 0.15 mg/ml. The solution was sprayed onto the substrate surface using the Sono-Tek ExactaCoat system equipped by the Impact spray nozzle. Schematic drawing of the application process is shown in Figure 1. Spray nozzle travel rate over the substrate was set to 100 mm/s. Nozzle height above the sample was 60 mm. Nozzle travel path above the substrate surface had a form of a meander in 15 mm steps. The amount of applied solution was 0.3 ml/cm^2, which was equivalent to the iron film thickness on the substrate equal to 8 nm. Heating table temperature was set to 230°C. The choice was conditioned by the temperature at which iron nitrate is fully decomposed to $Fe_4O_2(OH)_4$ [10].

2.2. PECVD synthesis

CNT arrays were grown in a PECVD reactor. Synthesis was conducted in the following conditions:

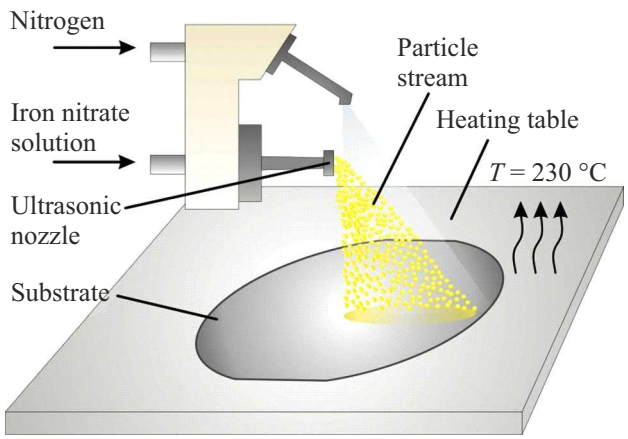

Figure 1. Schematic drawing of application of the $Fe(NO_3)_2 \cdot 9H_2O$ solution in isopropyl alcohol.

Characteristics of the lines used for calculations

Therm	λ (Å)	$h\nu_{ki}$, eV	A_{ki}	g_{ki}	$A_{ki}g_{ki}\nu_{ki}$
$1S^5$	7067	1.733	3.8	5	33.61
	8015	1.545	9.3	5	71.89

argon flow rate $(Ar) = 50\,cm^3/min$, ammonia flow rate $(NH_3) = 25\,cm^3/min$, acetylene flow rate $(C_2H_2) = = 50\,cm^3/min$,helium flow rate $(He) = 2.1\,cm^3/min$. The process temperature was $T = 750°C$. Plasma power was $R_f = 150\,W$ and remained constant. Conditions for each series of experiments were set as follows: synthesis conditions were not changed, except the hydrogen flow rate in the system. Varying flow rates are given below. Each experiment consisted of 4 stages: 1) substrate heating with the applied catalyst layer; 2) catalyst film oxidation in oxygen; 3) catalyst recovery in ammonia and hydrogen flows; 4) synthesis. Oxygen was fed into the reaction zone with the catalyst at the oxidation stage, the recovery stage was accompanied by hydrogen supply. These stages are required for formation of catalyst clusters on the Si substrate for CNT synthesis.

3. Sample examination and plasma temperature measurement techniques

Morphology of the obtained CNT was examined using the scanning and high-resolution transmission electron microscopy (JEOL JEM-2100Plus). Qualitative analysis of the CNT was performed using the Raman scattering spectroscopy (RSS). A 532 nm laser was used for RS spectra excitation. Spectral resolution was lower than $0.5\,cm^{-1}$. Diffraction grating had 1200 lines/mm^2.

Plasma temperature is an important PECVD parameter. This temperature was calculated using the argon plasma radiation spectra. A line intensity ratio method was chosen in this case [11]. Figure 2 shows optical transitions between two spectral lines with the common lower level, $l \to i$ and $k \to i$.

Plasma temperature was calculated as follows [11]:

$$T_p = \frac{h(\nu_{li} - \nu_{ki})}{k \ln(\frac{I_{ki}A_{li}\nu_{li}g_l}{I_{li}A_{ki}\nu_{ki}g_k})}, \quad (1)$$

where A_{ki} is the transition probability, ν_{ki} are transition frequencies, h is the Planck constant, I_{ki} and I_{li} are the spectral line intensities, g_l and g_k are degeneracy factors of particular states.

The calculations used lines, whose characteristics are listed in the table. Transition intensities were determined using argon plasma radiation. Plasma temperatures were calculated for each experiment that was always accompanied with radiation spectra measurements.

For CNT arrays grown at different hydrogen flow rates (25, 50 and 100 cm^3/min), Raman scattering (RS) spectra were measured during the synthesis. Two lines D $(1350\,cm^{-1})$ and G $(1580\,cm^{-1})$ were observed on all RS spectra. It is known that the intensity ratio of these bands (I_D/I_G) is used for numerical rating of the mean defect level of a CNT array [12]. Intensity ratio I_D/I_G for each experiment was: 0.846 without hydrogen; 1.176 at H_2 flow rate equal to 25 cm^3/min; 1.435 at H_2 flow rate equal to 50 cm^3/min and 1.786 at H_2 flow rate equal to 100 cm^3/min. These dependences of I_D/I_G on the hydrogen low rate are shown in Figure 3. A sample synthesized without hydrogen supply has the best I_D/I_G. Thus, a conclusion may be made that with an increase in hydrogen content during the synthesis, CNT defect level increases.

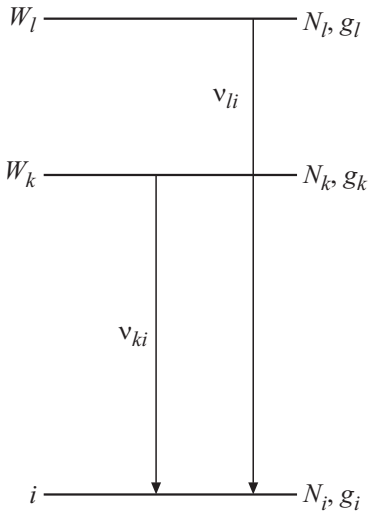

Figure 2. Diagram of optical transitions with one ground level and two excited levels.

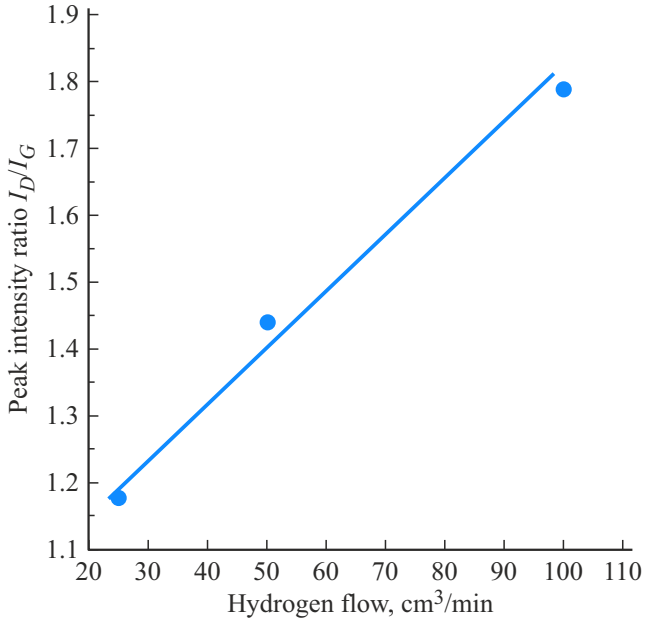

Figure 3. Dependence of the RSS peak intensity ratio on the hydrogen flow rate.

Optical spectral measurement of plasma was used to determine plasma temperature. As the H_2 flow rate increased, the plasma temperature decreased. At the same time, line intensity associated with C−H radicals increases in the plasma spectra as expected, and the C−C line intensity decreases, which is associated with the interaction between hydrogen and carbon.

4. Gas-discharge hydrocarbon pyrolysis thermodynamics

Atomic carbon fugacity in the catalyst substance is an important CNT growth property. This particular carbon is involved in the nanotube growth. Let's calculate this quantity during plasma-chemical pyrolysis processes. Taking into account the complexity of running processes and large number of reactions, the calculations used the Gibbs free energy minimization method [13,14] to consider the whole variety of processes.

This method implies that there is an equilibrium in the system: temperature and pressure are aligned, all kinetic processes became stationary. In this case, when the temperature and pressure are constant, the Gibbs free energy shall be minimized:

$$G = H - TS.$$

Calculation algorithm is in the analysis of free system energy components. Then, this energy is minimized using additional conditions, with conservation laws serving as such conditions.

4.1. Conservation laws in hydrocarbon pyrolysis

Conservation laws are defined by particle and molecule balance in the system. The number of atoms in each of the substances is denoted by the subscript N_α. Subscript „α" corresponds to a simple substance atom. Subscript „k" will be used for compounds. This subscript is defined as any compound regardless of its composition. The number of molecules of the same kind in a compound, which is only in the gas phase, is denoted by N_k. The number of positions will be denoted by a superscript. Therefore, the number of positions for a simple substance and compounds will be N^α and N^k, respectively. The number of particles in the system is defined by saturating vapor pressure at the given temperature. This tabular quantity may be found from a phase diagram of the given type of gas.

$$N^\alpha = p_{as}/kT, \quad N^k = p_{ks}/kT. \tag{2}$$

The total number of positions in the gas phase is defined by the sum of quantities set by expressions:

$$N = \sum_\alpha p_{as}/kT + \sum_k p_{ks}/kT = \sum_\alpha N^\alpha + \sum_k N^k. \tag{3}$$

The number of positions may be calculated using the saturating vapor pressure consisting completely from a particular kind of gas molecules. The number is equal to the number of chemical components of the system, and a position number conservation law might be written for each of them.

For simple substances:

$$\varphi^\alpha = N^\alpha - N_\alpha - N^0_\alpha = 0, \tag{4}$$

and for carbon compounds:

$$\varphi^k = N^k - N_k - N^0_k = 0, \tag{5}$$

where $N^0_{\alpha,k}$ is the number of positions in the gas phase that remain free.

Carbon molecules may bind together and make new compounds. These complex objects, in terms of thermodynamics, may be described in a common way. In addition, atoms and molecules of each substance may be in free and ionized state. The number of carbon atoms forming particular ions is denoted by: $N_{\alpha q}$. Subscript q, that denotes charge states, may take on discrete values. Thus, for example, for ionization of a double-charged molecule, this subscript takes on two values „0" and „+1", or „0" and „−1". For a multiply ionized molecule, this subscript covers a wider range of values. The number is equal to the number of molecule charge states. The „charge state" concept makes it possible to treat positively and negatively charged ions, singly and multiply ionized molecules in a common way.

An atom of each element may be in a free state or as part of a compound. In pyrolysis the composition of compounds and number of free nitrogen atoms and other substances may vary, but their sum remains unchanged due to the system closedness. This position is the basis for writing the law of conservation of a particular kind of atoms and molecules:

$$\varphi_\alpha = N_\alpha - \sum_{\alpha q} N_{\alpha q} - \sum_{\alpha,k} N_k m_{\alpha k} = 0,$$

$$\varphi_k = N_k - \sum_{kq} N_{kq} = 0. \tag{6}$$

Here, m_α is the number of simple substance (carbon or hydrogen) atoms in a hydrocarbon molecule.

Plasma quasi-neutrality condition requires the balance of positive and negative charges, i.e.: fulfilment of the charge conservation law:

$$\varphi_e = n - \sum_{\alpha q} q_\alpha N_{\alpha q} - \sum_{q,k} q_k N_k = 0. \tag{7}$$

Note also that (q) may be both positive and negative. Both single atoms and compounds may be ionized, which is also considered in equation (7) written in the most general form.

4.2. Free energy of the system

The system's Gibbs free energy is written as:

$$G = G^G(N^G_{\alpha q}, N_{kq}) + G^e, \tag{8}$$

where G^G is the free gas phase energy; $N_{\alpha q}$ is the concentration of α atoms in the gas phase that are in the

charge state q; N_{kq} is the concentration of compounds in a particular charge state; G^e is a free energy of electronic subsystem, to which all charge-carrying elements, both atoms and molecules, contribute.

To find an explicit view of the dependence of free energy on the concentration of atoms and molecules, the partial Gibbs potential is introduced per a compound atom or molecule:

$$g_{\alpha q} = g_\alpha = H_\alpha - TS_\alpha,$$

$$g_{kq} = g_k = H_k - TS_k + \sum_{\alpha kq} m_{\alpha k}(H_k - TS_k), \qquad (9)$$

where $H_{\alpha(k)}$ is the free energy of formation of a neutral atom (compound), $S_{\alpha(q)}$ is the vibrational (heat) entropy associated with the atom (compound), $\varepsilon_{\alpha(k)q}$ is the energy to be spent to put an atom (compound) into the charge state q. Equation (9) accounts for formation of compounds from single atoms. For space considerations, brackets are used in notations: α — is related to an atom, and (k) in brackets relates to a compound. In equations (9), they are given separately.

Heat portion of free energy is calculated as a sum of a product of partial free energies of atoms and molecules by their concentration:

$$G_T = \sum_\alpha g_\alpha N_\alpha + \sum_k g_k N_k + G^e. \qquad (10)$$

Configuration portion of free energy is expressed by the Boltzmann constant:

$$G_K = -kT \ln W, \qquad (11)$$

where W is the thermodynamic probability of state (number of macroscopic state implementation methods).

$$W = \prod_{\alpha,k} \frac{N^\alpha!}{N_{\alpha q}!(N^\alpha - N_\alpha!\left(N_\alpha - \sum\limits_q N_{\alpha q}\right)!} \times \frac{N^k!}{N_{kq}!(N^k - N_k!\left(N_k - \sum\limits_q N_{kq}\right)!} \qquad (12)$$

considers all permutation of identical atoms and compounds with respect to their places and of charge states with respect to their elements. The total number of particles of the same kind in the system:

$$N_\alpha = \sum_{\alpha,q} N_{\alpha q} + \sum_{\alpha,k,q} N_{kq} m_{\alpha k}. \qquad (13)$$

Free energy of an electronic subsystem may be written as:

$$G^e = \sum_{\alpha,q} N_{\alpha q}\varepsilon_{\alpha q} + \sum_{k,q} N_{kq}\varepsilon_{kq}. \qquad (14)$$

Electrons in the system result from atom and molecule ionization, therefore the charge conservation law is written as:

$$\varphi_e = n - \sum_{\alpha,q} qN_{\alpha q} - \sum_{k,q} qN_{kq}. \qquad (15)$$

Equilibrium concentration of carbon and hydrogen atoms and compounds formed during the pyrolysis is found by the Lagrange multiplier method. Equilibrium in the system corresponds to the functional minimum:

$$\Psi = G_T + G_K + \sum_\alpha \lambda_\alpha \varphi_\alpha + \sum_\alpha \lambda^\alpha \varphi^\alpha + \lambda_e \varphi_e + \sum_k \lambda_k \varphi_k + \sum_k \lambda^k \varphi^k. \qquad (16)$$

Final expression for the free energy functional will be written as:

$$\begin{aligned}\Psi = {} & \sum_\alpha g_\alpha N_\alpha + \sum_k g_k N_k + \sum_{\alpha,q} N_{\alpha q}\varepsilon_{\alpha q} + \sum_{k,q} qN_{kq}\varepsilon_{kq} \\ & - kT \ln \prod_{\alpha,k} \frac{N^\alpha!}{\prod_\alpha N_{\alpha q}!(N^\alpha - N_\alpha)!(N_\alpha - \sum_q N_{\alpha q})!} \\ & \times \frac{N^k!}{\prod_k N_{kq}!(N^k - N_k)!(N_k - \sum_q N_{kq})!} \\ & + \lambda^p\left(N - \sum_\alpha N^\alpha - \sum_k N^k\right) \\ & + \sum_{\alpha,k,q} \lambda_\alpha\left(N_\alpha - \sum_{\alpha,q} N_{\alpha q} - \sum_{\alpha,k} N_k m_{\alpha k}\right) \\ & + \lambda_e\left(n - \sum_{\alpha,q} q_\alpha N_{\alpha q} - \sum_{q,k} q_k N_{kq}\right) + \lambda_k \sum_{q,k}\left(N_k - \sum_{kq} N_{k,q}\right) \\ & + \lambda^k \sum_k (N^k - N_k - N_k^0) + \lambda^\alpha \sum_\alpha (N^\alpha - N_\alpha - N_\alpha^0). \end{aligned} \qquad (17)$$

In accordance with the Fermi level determination (chemical potential of an electron), we find the sense of the multiplier λ_e:

$$E_\mathrm{F} = \frac{\partial G}{\partial n} = \frac{\partial \Psi}{\partial n} = \lambda_e. \qquad (18)$$

This Lagrange multiplier coincides with the Fermi level energy.

Derivative of free energy with respect to the number of atoms of a substance or the number of molecules is a chemical potential, consequently, dislocating molecules are in equilibrium with atoms that appear during pyrolysis. Therefore, the chemical potential of these free atoms and atoms in the molecule are equal because a thermodynamic equilibrium takes place in the system. Thus, the following condition takes place for each kind of particles: $\mu_\alpha^g = \mu_\alpha^{mol}$, where μ_α^g is the chemical potential of an atom in the gas phase, μ_α^{mol} is the chemical potential of an atom in a molecule.

$$\mu_\alpha^{mol} = \mu_\alpha^0 + \ln m_{k\alpha} x_{k\alpha} \approx \mu_\alpha^0 + \ln m_{k\alpha} f_{k\alpha}, \qquad (19)$$

where $x_{k\alpha}$ is the concentration in the gas phase of molecules, pyrolysis of which gives rise to α type atoms; $f_{k\alpha}$ is the fugacity of these molecules.

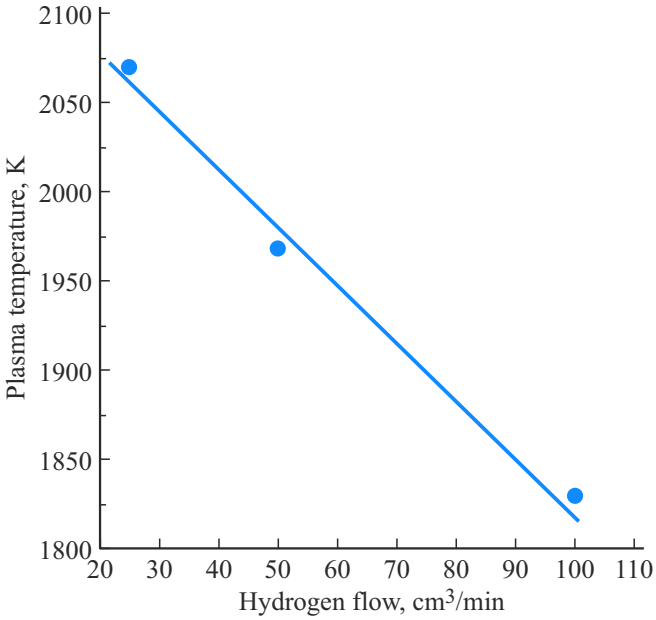

Figure 4. Dependence of plasma temperature on hydrogen flow.

By differentiating Ψ with respect to N^{α}, we get the correlation between the Lagrange multiplier and concentrations:

$$\lambda_{\alpha} = -kT \ln N^{\alpha} + kT \ln(N^{\alpha} - N_{\alpha}). \quad (20)$$

By differentiating Ψ with respect to N_{α}, we get that the chemical potential of α elements in the gas phase is expressed in terms of the Lagrange multipliers of the position and particle conservation law:

$$\lambda_{\alpha} = \mu_{\alpha}^{0} + \ln m_{k\alpha} f_{k\alpha} - \left[g_{\alpha} + kT \ln\left(N_{\alpha} - \sum_{q} N_{q\alpha}\right) - kT \ln(N^{\alpha} - N_{\alpha}) \right]. \quad (21)$$

A common representation for the chemical potential is used here: $\mu_{\alpha}^{0} + kT \ln a$, μ_{α}^{0} chemical potential of nitrogen in standard conditions.

A derivative of Ψ with respect to $N_{q\alpha}$ is taken. The following is obtained as a result of calculations:

$$N_{q\alpha} = N^{\alpha} kT \frac{(p_0)^m N^{C_n H_m}}{p_{C_n H_m} (p_H^g)^m} \exp\left(-\frac{g_{\alpha} + \varepsilon_{q\alpha} - \mu_{\alpha}^{0} - q_{\alpha} E_{\mathrm{F}}}{kT}\right) = f_{k\alpha} N^{\alpha} \exp\left(-\frac{E_a - q_{\alpha} E_{\mathrm{F}}}{kT}\right), \quad (22)$$

where $E_{\alpha} = g_{\alpha} + \varepsilon_{q\alpha} - \mu_{\alpha}^{0}$ is the energy of activation of conventional, rather than plasma-chemical, pyrolysis.

Carbon solubility in a catalyst may be calculated using equations describing the Fe–C phase diagram solidus. This calculation is described in [14]. The calculation gives:

$$X_{\mathrm{C}}^{\mathrm{Fe}} = \frac{a_{\mathrm{C}}^{\mathrm{Fe}}}{\gamma_{\mathrm{C}}^{Ft}} = \left[kT \frac{(p_0)^m N^{C_n H_m}}{p_{C_n H_m} (p_H^g)^m} \times \exp\left(-\frac{g_{C_n H_m} - m\mu_H^0 - n\mu_C^0 - q_C E_{\mathrm{F}}}{kT}\right)\right]^{1/n} \times \exp\left(-\frac{\Omega(1 - X_{\mathrm{C}}^{\mathrm{Fe}})}{kT}\right). \quad (23)$$

Two factors affect the carbon activity in the catalyst. Firstly, the partial pressure of hydrogen is in the denominator of this equation. As the partial pressure grows, carbon solubility in the catalyst decreases. Secondly, the plasma temperature decreases as the hydrogen flow rate in the reactor grows (Figure 4). E_{F} is linearly related to the reduction of gas-phase pyrolysis energy. Pyrolysis energy reduction is induced by gas heating in plasma discharge.

$$E_{\mathrm{F}} = kT_p. \quad (24)$$

According to the experimental data, the plasma temperature decreases as the total reactor pressure grows. E_{F} decreases, but the nominator of exponent in equation (23) grows, also giving rise to a decrease in the carbon activity in the catalyst. Accordingly, the amount of carbon fed into the growing nanotube decreases. This gives rise to a growth of defect level (Figure 3).

5. Conclusion

The study involved experimental investigations of CNT growth in has discharge plasma with different hydrogen flow rates. The experiment shows that as the hydrogen flow rate grows, the nanotube defect level evaluated from I_D/I_G also increases. Defect level growth takes place notwithstanding that hydrogen actively restores the catalyst by removing pyrolysis product impurities. This is proved by the growth of plasma radiation band intensity corresponding to the presence of C–H radicals. Analysis of the gas-phase pyrolysis thermodynamics facilitates the explanation of the experimental fact and identifies two reduction factors of carbon activity in the catalyst, i. e. direct hydrogen pressure growth and plasma temperature reduction with hydrogen flow rate growth.

Funding

The study was supported by the Ministry of Science and Higher Education of the Russian Federation, project FFFG-2025-0002, using the Large Scale Research Facility Complex for Heterogeneous Integration Technologies and Silicon + Carbon Nanotechnologies at the Institute of Nanotechnology of Microelectronics of the Russian Academy of Sciences.

Conflict of interest

The authors declare that they have no conflict of interest.

References

[1] S. Morais. Nanomaterials (Basel, Switzerland) **13**, 19 (2023). https://doi.org/10.3390/nano13192674.
[2] F.U. Siddiqui, S. Rathore. Int. J. Mech. Eng. Technol. **14**, *5*, 1 (2023).
[3] S.V. Bulyarskiy, A.A. Dudin, A.V. Lakalin, A.P. Orlov, A.A. Pavlov, R.M. Ryazanov, A.A. Shamanaev. Tech. Phys. **63**, *6*, 894 (2018). https://doi.org/10.1134/S1063784218060099.
[4] K.L. Jensen, D.A. Shiffler, J.R. Harris, I.M. Rittersdorf, J.J. Petillo. J. Vac. Sci. Technol. B **35**, 2 (2017). https://doi.org/10.1116/1.4968007.
[5] M. Mauger, V.T. Binh. J. Vac. Sci. Technol. B **24**, *2*, 997 (2006). https://doi.org/10.1116/1.2179454.
[6] D. Li, L. Tong. Processes **9**, *1*, 36 (2021). https://doi.org/10.3390/pr9010036.
[7] S.-I. Jo, B.-J. Lee, G.-H. Jeong. J. Korean Phys. Soc. **76**, *12*, 1110 (2020). https://doi.org/10.3938/jkps.76.1110.
[8] P. Ji, J. Chen, T. Huang, L. Zhuge, X. Wu. Diam. Relat. Mater. **109**, 108067 (2020). https://doi.org/10.1016/j.diamond.2020.108067.
[9] D. Mariotti, Y. Shimizu, T. Sasaki, N. Koshizaki. J. Appl. Phys. **101**, 1 (2007). https://doi.org/10.1063/1.2409318.
[10] P. Melnikov, V.A. Nascimento, I.V. Arkhangelsky, L.Z. Zanoni Consolo, L.C.S. de Oliveira. J. Therm. Anal. Calorim. **115**, *1*, 145 (2014). https://doi.org/10.1007/s10973-013-3339-1.
[11] V.I. Gorbunkov, V.V. Kositsyn, V.I. Ruban, V.V. Shalai. Omsky nauchny vestnik. Seriya: Aviatsionno-raketnoe i energetich-eskoe mashinostroenie **2**, *3*, 44 (2018). (in Russian). https://doi.org/10.25206/2588-0373-2018-2-3-44-50.
[12] A. Thapa, Y.R. Poudel, R. Guo, K.L. Jungjohann, X. Wang, W. Li. Carbon **171**, 188 (2021). https://doi.org/10.1016/j.carbon.2020.08.081.
[13] S.V. Bulyarskii, V.P. Oleinikov. Physica Status Solidi B **146**, *2*, 439 (1988). https://doi.org/10.1002/pssb.2221460204.
[14] S.V. Bulyarski, V.V. Fistul. Termodinamika i kinetika vza-imodeistvuyushchikh defektov v poluprovodnikakh. Fizmatlit, Moskva, (1997). 351 s. (in Russian).

Translated by E.Ilinskaya